

Field-Induced Non-BEC Transitions in Frustrated Magnets

Shouvik Sur¹, Yi Xu¹, Shuyi Li¹, Shou-Shu Gong², and Andriy H. Nevidomskyy¹

¹*Department of Physics and Astronomy, Rice University, Houston, Texas 77005, USA*

²*School of Physical Sciences, Great Bay University, Dongguan 523000, China,
and Great Bay Institute for Advanced Study, Dongguan 523000, China*

 (Received 6 July 2023; revised 12 December 2023; accepted 4 January 2024; published 5 February 2024)

Frustrated spin systems have traditionally proven challenging to understand, owing to a scarcity of controlled methods for their analyses. By contrast, under strong magnetic fields, certain aspects of spin systems admit simpler and universal description in terms of hardcore bosons. The bosonic formalism is anchored by the phenomenon of Bose-Einstein condensation (BEC), which has helped explain the behaviors of a wide range of magnetic compounds under applied magnetic fields. Here, we focus on the interplay between frustration and externally applied magnetic field to identify instances where the BEC paradigm is no longer applicable. As a representative example, we consider the antiferromagnetic J_1 - J_2 - J_3 model on the square lattice in the presence of a uniform external magnetic field, and demonstrate that the frustration-driven suppression of the Néel order leads to a Lifshitz transition for the hardcore bosons. In the vicinity of the Lifshitz point, the physics becomes unmoored from the BEC paradigm, and the behavior of the system, both at and below the saturation field, is controlled by a Lifshitz multicritical point. We obtain the resultant universal scaling behaviors, and provide strong evidence for the existence of a frustration and magnetic-field driven correlated bosonic liquid state along the entire phase boundary separating the Néel phase from other magnetically ordered states.

DOI: [10.1103/PhysRevLett.132.066701](https://doi.org/10.1103/PhysRevLett.132.066701)

Introduction.—Bose-Einstein condensates and superfluids are the most generic ground states of repulsively interacting, dense Bose gases above one dimension [1]. For bosons hopping on a lattice, additional possibilities, such as Mott insulating phases, become possible at strong repulsive interactions [2]. It has been suggested that, under suitable conditions, interacting bosons may also exist in a symmetric quantum-liquid state—a Bose metal, which is stabilized by an interplay between interactions and an enhanced low-energy density of states (DOS) [3,4]. Over the past decades, the latter property has been utilized for stabilizing other kinds of Bose liquid states in Rashba spin-orbit coupled bosons [5], deconfined critical points between valence bond solids [6], superfluid phases in the dipolar Bose-Hubbard model [7], certain tensor gauge theories [8], and fractonic superfluids [9]. Unlike their fermionic counterparts, pure bosonic systems are comparatively rare in nature. It is, therefore, important to identify new platforms which may support unconventional phenomenology of bosonic systems.

Because of the connection between localized spins and bosons, frustrated magnets are promising candidates for realizing unconventional bosonic matter. Frustrated magnetic systems, however, pose significant challenges to a theorist, owing to a scarcity of controlled approaches, especially for low-spin systems [10,11]. A rare avenue becomes available in the presence of a uniform magnetic field—since all spins in any quantum magnetic system will

polarize when exposed to a sufficiently strong magnetic field, quantum fluctuations are suppressed in the vicinity of the resultant field-polarized (FP) state. In this region, the system can be mapped to a dilute gas of interacting bosons [12], and frustration manifests itself in the bosonic band structure. Indeed, much of the conventional phenomenology of interacting dilute Bose gases has been realized in such magnetic systems, including BEC, superfluidity, and Mott transition [13,14]. Since the degree of frustration acts as an additional nonthermal tuning parameter, it introduces the possibility of realizing unconventional states of bosonic matter [15–18], which bear similarities with those proposed in spin-orbit coupled bosonic systems [19,20]. In this Letter, we focus on the vicinity of multicritical points that arise at the intersections of frustration-driven and magnetic-field-driven continuous phase transition lines. While frustration tends to stabilize quantum paramagnetic states, a high magnetic field nearly saturates the spins. As we shall show, the combined effect of the two nonthermal agents facilitates a controlled access to Bose liquid states in frustrated magnets under an applied magnetic field, which are analogs of Bose metals and have remained unexplored in this context.

The zero-temperature transition between an FP and a magnetically ordered state is expected to be continuous, whereby the spin-rotational symmetry perpendicular to the field-polarization direction is spontaneously broken. The transition belongs to the “BEC universality class,” which is

characterized by the dynamical critical exponent $z = 2$ [21]. Extensive experiments on antiferromagnets and quantum paramagnets have established the importance of BEC-based perspective in understanding the physics of a wide variety of magnetic compounds under applied magnetic fields [22–39]. In this Letter, we propose scenarios where this conventional outcome breaks down. In particular, we establish (i) transitions that go beyond the BEC universality class, and (ii) explore the possibility of emergent Bose metallic physics in spin systems exposed to strong magnetic fields. We expect our results to be relevant to frustrated magnets with signatures of spin-liquid correlations under high magnetic fields [40–43].

Model and phase diagram.—We consider a spin- $\frac{1}{2}$ Heisenberg model on the square lattice with antiferromagnetic interactions beyond nearest-neighbor,

$$H_0 = J_1 \sum_{\langle rr' \rangle} \vec{S}_r \cdot \vec{S}_{r'} + J_2 \sum_{\langle\langle rr' \rangle\rangle} \vec{S}_r \cdot \vec{S}_{r'} + J_3 \sum_{\langle\langle\langle rr' \rangle\rangle\rangle} \vec{S}_r \cdot \vec{S}_{r'}, \quad (1)$$

where all $J_n > 0$, and \vec{S}_r represents the three-component spin-1/2 operator at site r . We employ J_1 as the overall energy scale, and define dimensionless ratios $\tilde{X} = X/J_1$ for any quantity X that possesses the dimension of energy. The classical phase diagram, obtained by analyzing Luttinger-Tisza (LT) bands [44], is presented in Fig. 1(a). For $\tilde{J}_2 + 2\tilde{J}_3 < 1/2$ a Néel antiferromagnet (AFM) is realized. In the complement of this region, classically, various spiral and stripe ordered phases are expected. The transitions between Néel and spiral ordered phases are expected to be second order, with a continuous evolution of the ordering wave vector (see, e.g., Ref. [45]), which manifest themselves as Lifshitz transitions of the LT band structure. The corresponding critical points lie along the line $\tilde{J}_2 + 2\tilde{J}_3 = 1/2$ with $\tilde{J}_3 > 0$, henceforth labeled as “critical line 1” (CL₁) [46]. Because of the enhanced DOS on CL₁, quantum fluctuations may be expected to suppress magnetic order in its vicinity [47–50]. Recent numerical simulations support this expectation, and quantum spin-liquid states have been reported in the vicinity of CL₁ [51–53].

We introduce a uniform magnetic field B such that the system is governed by $H(h) = H_0 - h \sum_r S_r^{(z)}$, where $h := g\mu_B B$ is the Zeeman field with g and μ_B denoting the Landé g -factor and Bohr magneton, respectively. The magnetic field tends to polarize the spins along the \hat{z} direction, and cants the AFM order. At sufficiently high fields ($h > h_c$ with h_c being the saturation field), the canted AFM phases give way to FP states, which are classical ground states with all spins polarized along the magnetic field direction (\hat{z}). A constant- \tilde{J}_3 slice of the resultant phase diagram in the large- S limit is depicted in Fig. 1(b). In this Letter, we focus on the neighborhood of the transition between the canted AFM and FP phases. In particular, we

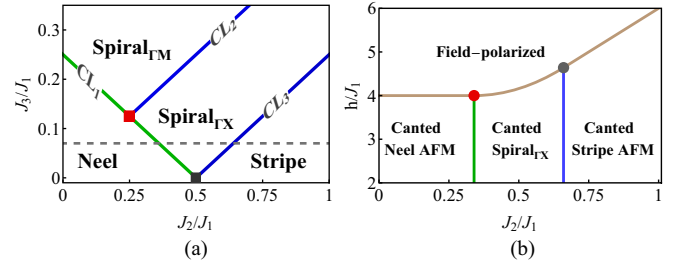


FIG. 1. Phase diagrams in the absence and presence of an externally applied magnetic field (h). (a) Classically, at $h = 0$, four antiferromagnetic phases are obtained, which are separated by critical lines (CL _{n}). (b) These phases develop canting with h , before continuously transitioning to field-polarized states at sufficient high $h > h_c$ (brown curve). Multicritical points (filled squares and circles) are obtained at the intersection of all critical lines. The phase boundaries in (b) are obtained from a linear spin-wave analysis at a fixed J_3/J_1 [dashed line in (a)].

ask how the transition is affected by the Lifshitz criticality along CL₁. We formulate a scaling theory for the multicritical points at the intersection of the saturation-field surface and CL₁ [see Fig. 1(b)], and demonstrate the existence of magnetic field-tuned transitions belonging to a non-BEC universality class for *all* points on CL₁. These non-BEC critical points strongly affect the phase diagram in their vicinity, most remarkably through the stabilization of a quantum-liquid state at subcritical fields.

Non-BEC transitions.—In the vicinity of h_c , spin fluctuations may be conveniently modeled by density and phase fluctuations of hardcore bosons through the Matsubara-Matsuda transformation [54,55], $S_r^{(+)} \rightarrow b_r^\dagger$; $S_r^{(-)} \rightarrow b_r$; $S_r^{(z)} \rightarrow \frac{1}{2} - \rho_r$. Thus, we rephrase the problem in terms of the hardcore bosons b_r , with ρ_r being their local density. The Hamiltonian acquires the form of a Bose-Hubbard model on the square lattice

$$H(h) = \int \frac{d^2\mathbf{K}}{(2\pi)^2} [\mathcal{E}(\mathbf{K}) - \mu(h)] b(\mathbf{K})^\dagger b(\mathbf{K}) + \int \frac{d^2\mathbf{Q}}{(2\pi)^2} V(\mathbf{Q}) \rho(-\mathbf{Q}) \rho(\mathbf{Q}) + U \sum_r n_r (n_r - 1), \quad (2)$$

where the last term enforces the hardcore condition in the limit $U \rightarrow \infty$ [55]. The “chemical potential,” $\mu(h) = \sum_{i=1}^3 J_i - h$, tuned by h , controls the average density of bosons. The dispersion $\mathcal{E}(\mathbf{K})$ and the coupling function $V(\mathbf{Q})$ are independent of h , but sensitive to the J_n ’s [44]. In particular, $\mathcal{E}(\mathbf{K})$ tracks the LT band structure, and reflects the singularities at the classical phase boundaries: at a fixed \tilde{J}_3 and as a function of \tilde{J}_2 , the boson band undergoes Lifshitz transitions as the critical lines are crossed [56]. We note that XXZ anisotropies, if present, can be absorbed in $V(\mathbf{Q})$.

In the Néel AFM phase the dispersion is minimized at the M point of the BZ. Thus, the long-wavelength

fluctuations of the bosons Φ carry momenta in the vicinity of the M point, and the low-energy effective theory governing these fluctuations is given by $S_M = \int d\tau d\mathbf{r} \mathcal{L}_M[\Phi(\tau, \mathbf{r})]$ with

$$\mathcal{L}_M[\Phi] = \Phi^*[\partial_\tau + \varepsilon(\nabla) - \mu_{\text{eff}}]\Phi + g|\Phi|^4, \quad (3)$$

where we have expanded the dispersion as $\mathcal{E}((\pi, \pi) + \mathbf{k}) = -\mathcal{E}_0 + J_1\varepsilon(\mathbf{k})$ such that $\varepsilon(\mathbf{k}) \geq 0$, and defined the effective parameters $\mu_{\text{eff}} = J_1(\tilde{h}_c - \tilde{h})$ with $\tilde{h}_c = (3 - \tilde{J}_2 - \tilde{J}_3)$, and $g := \tilde{V}(\mathbf{Q} = \mathbf{0}) = 2(1 + \tilde{J}_2 + \tilde{J}_3)$. The magnetic field-driven transition can be understood as a transition between a state with no bosons (an FP state; $\mu_{\text{eff}} < 0 \equiv h > h_c$) to a state with a finite density of bosons ($\mu_{\text{eff}} > 0 \equiv h < h_c$). The transition itself is described with respect to the critical point at $\mu_{\text{eff}} = 0 \equiv h = h_c$. If a magnetic long-range order is present for $h < h_c$, the bosons develop an off-diagonal long-range order (ODLRO), which implies a BEC state [1,57] with $\langle \Phi \rangle \neq 0$. As CL_1 is approached from the Néel AFM side of the phase diagram, does the field-driven transition continue to be described by the BEC universality class?

We answer this question by first noting the dispersion about the band minimum in the vicinity of CL_1 ,

$$\varepsilon(\mathbf{k}, m_L) = m_L|\mathbf{k}|^2 + A \cos \gamma (k_x^4 + k_y^4) + 2A \sin \gamma k_x^2 k_y^2, \quad (4)$$

where the ‘‘Lifshitz mass’’ $m_L = (1/2 - \tilde{J}_2 - 2\tilde{J}_3)$, and the parameters $A = \frac{1}{24} \sqrt{36\tilde{J}_2^2 + (2\tilde{J}_2 + 16\tilde{J}_3 - 1)^2}$ and $\gamma = \tan^{-1} \{6\tilde{J}_2 / (2\tilde{J}_2 + 16\tilde{J}_3 - 1)\}$ [44]. In the parameter regime where $m_L > 0$, the field-driven transition belongs to the BEC universality class. As CL_1 is approached, $m_L \rightarrow 0$ and the field-driven transition belongs to a distinct universality class that is controlled by the Lifshitz multicritical point (LMCP) at $h = h_c$ and $\tilde{J}_2 = \tilde{J}_{2c}$. At the LMCP, although $\mu_{\text{eff}} = 0$, strong quantum fluctuations arise in the presence of interactions among bosons, owing to the divergent DOS. Consequently, V_{eff} becomes strongly relevant at the Gaussian fixed point governed by the first term in Eq. (3). This strong coupling theory, however, is exactly solvable at $T = 0$, due to the absence of particle-hole excitations [12,21,58]. In particular, the positive semidefiniteness of $\varepsilon(\mathbf{q})$ leads to a chiralitylike constraint on the bosonic dynamics, which protects the quadratic terms in the action against quantum corrections [44,59]. This is analogous to chiral fermionic liquids, where tree-level or classical critical exponents remain robust against quantum fluctuations, thanks to the chiral dynamics [60,61]. Thus, in the present case, the tree-level critical exponents

$$z = 4; \quad \nu_h = 1/4; \quad \nu_J = 1/2; \quad \eta = 0, \quad (5)$$

do not accrue anomalous dimensions through quantum fluctuations [44]. Here, z is the dynamical critical exponent,

ν_h and ν_J control the scaling of the correlation length along h and J_2 axes, respectively, and η is the anomalous dimension of Φ . Since this is a multicritical point, the correlation length with respect to the LMCP is given by $\xi = 1/\sqrt{\xi_h^{-2} + \xi_J^{-2}}$ with $\xi_h \sim |h - h_c|^{-\nu_h}$ and $\xi_J \sim |J_2 - J_{2c}|^{-\nu_J}$. The critical exponents imply the magnetic field-driven transition at $J_2 = J_{2c}$ does not belong to the BEC universality class, which would have been characterized by $\xi \sim |h - h_c|^{-1/2}$.

In contrast to the particle-hole channel, nontrivial quantum fluctuations are present in the particle-particle channel, which drive the system toward an interacting fixed point. To see this, we perform Wilsonian renormalization group (RG) analysis at $d = 4 - \epsilon$, where d is the number of spatial dimensions. We obtain the following one-loop RG flow of the parameters in \mathcal{L}_M [44]:

$$\partial_\ell \bar{g} = \epsilon \bar{g} - \frac{f_g(\gamma) \bar{g}^2}{16\pi^2 A}, \quad \partial_\ell \bar{\mu} = 4\bar{\mu}, \quad \partial_\ell \bar{m}_L = 2\bar{m}_L, \quad (6)$$

where ℓ is the logarithmic length scale, $(\bar{g}, \bar{\mu}, \bar{m}_L) = (\Lambda^{-\epsilon} g, \Lambda^{-4} \mu_{\text{eff}}, \Lambda^{-2} m_L)$, Λ is the ultraviolet (UV) momentum cutoff, and $f_g(\gamma) = \int_0^1 dt [t^2 + (1-t)^2] \cos \gamma + 2(1-t)t \sin \gamma^{-1}$. Since the LMCP is a multicritical point, it has two independent relevant directions, $\bar{\mu}$ and \bar{m}_L . By maintaining multicriticality of the LMCP, i.e., setting the bare values $\bar{m} = 0 = \bar{\mu}$, we obtain a stable fixed point at $[\bar{g}_*, \bar{\mu}_*, \bar{m}_{L,*}] = \{16\pi^2 A f_g^{-1}(\gamma) \epsilon, 0, 0\}$. Extrapolating the result to $\epsilon = 2$, yields a fixed-point coupling $\bar{g}_* = 32\pi^2 A f_g^{-1}(\gamma)$, which is independent of the UV structure of the interaction vertex, such as XXZ anisotropies. Because of its dependence on A and γ , \bar{g}_* varies along CL_1 , as shown in Supplemental Material, Fig. S2 [44]. In particular, as the critical point at $(A, \gamma) = (\frac{1}{8}, \pi/2) \equiv (\tilde{J}_2, \tilde{J}_3) = (\frac{1}{2}, 0)$ is approached along CL_1 , $f_g(\gamma) \sim \ln[1/(\pi/2 - \gamma)] \gg 1$; consequently, the fixed point is pushed to weaker couplings, and the one-loop result appears to become more accurate as $\gamma \rightarrow \pi/2$.

Multicriticality and crossover behaviors.—The LMCP is an example of ‘‘zero-scale-factor universality,’’ and the scaling functions for all observables are completely determined by microscopic or bare parameters [21]. Here, we focus on finite-temperature properties within the multicritical cone emanating from the LMCP, as depicted in Fig. 2(a). The shape of the cone is controlled by the temperature scale, $T_* = \sqrt{T_{*,h}^2 + T_{*,J}^2}$ with $T_{*,h} \sim \xi_h^{-z} \sim |h - h_c|$ and $T_{*,J} \sim \xi_J^{-z} \sim |J_2 - J_{2c}|^2$. Although the density of bosons at $h = h_c(\tilde{J}_2)$ vanishes at $T = 0$, thermal fluctuations at $T > 0$ makes it finite. Therefore, we expect the magnetization at $T > 0$ would be suppressed below that in the FP state. Using a finite- T scaling analysis [21,62], we estimate the average boson density to scale as

$$\rho_0(T) \equiv \langle \rho(T) \rangle = T^{d/4} f_T(T_*/T), \quad (7)$$

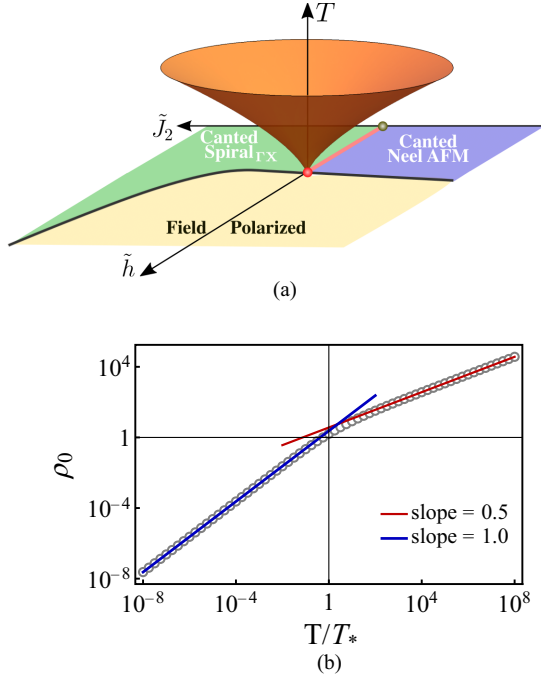


FIG. 2. Signatures of Lifshitz multicriticality. (a) The multicritical point (red dot) controls finite- T behaviors of the system within the (orange) critical cone. (b) Crossover behavior of ρ_0 with T [cf. Eq. (7)]. The circles (lines) are numerically evaluated values of ρ_0 (fits to the data). The unequal slopes indicate a crossover from $\rho_0 \sim T \rightarrow \sqrt{T}$. Here, T_* is the temperature scale associated with the cone in (a).

where the dimensionless function has the limiting behavior, $\lim_{x \ll 1} f_T(x) = \mathcal{O}(1)$ and $\lim_{x \gg 1} f_T(x) \sim 1/\sqrt{x}$. At the LMCP T_* vanishes, and only the former limit is applicable. In $d = 2$ this leads to $\rho_0(T) \equiv [1/2 - \langle S_r^{(z)} \rangle] \sim \sqrt{T}$. Away from the LMCP, but along the BEC transition line, $\rho_0(T)$ displays a crossover behavior. At low temperatures ($T \ll T_*$) the BEC critical points dictate the scaling and $\rho_0 \sim T$. At sufficiently high temperatures ($T \gg T_*$), however, the system enters the critical cone and $\rho_0 \sim \sqrt{T}$. This crossover behavior is depicted in Fig. 2(b).

The LMCP's influence on the phase diagram at subcritical fields can be understood in terms of the density and phase fluctuations of the bosons. While a finite mean-density reflects the deviation of $\langle S^{(z)} \rangle$ from $1/2$, phase fluctuations determine the correlation between $S^{(+)}$ and $S^{(-)}$. First, we consider the asymptotic behavior of the mean density in the region $0 < (1 - h/h_c) \ll 1$, which corresponds to $0 < \mu_{\text{eff}} \ll J_1$. From one-loop RG analysis, we obtain the scaling of the mean density with μ_{eff} ,

$$\rho_0(\mu_{\text{eff}}) = \mu_{\text{eff}}^{d/4} f_h(m_L^2/\mu_{\text{eff}}). \quad (8)$$

The dimensionless scaling function $f_h(x)$, is such that $\lim_{x \ll 1} f_h(x) = \mathcal{O}(1)$ and $\lim_{x \gg 1} f_h(x) \sim 1/\sqrt{x}$. Therefore,

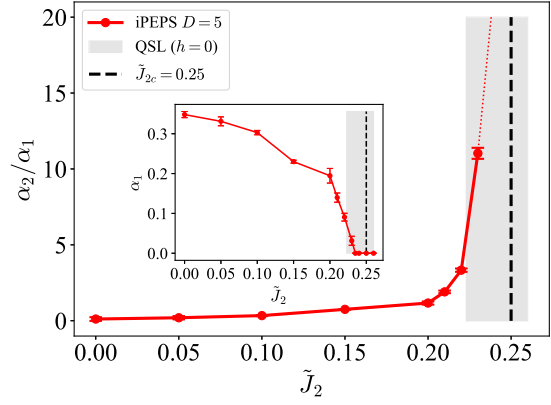


FIG. 3. Crossover in the scaling of $[1/2 - \langle S^{(z)} \rangle]$ with $\Delta h := (h_c - h)$ with increased frustration, obtained from iPEPS simulations. The data are fitted to the function, $[1/2 - \langle S^{(z)} \rangle] = \alpha_1 \Delta h \ln(h_c/\Delta h) + \alpha_2 \sqrt{\Delta h}$. Deep in the Néel phase the transition belongs to the Bose-Einstein-condensation universality class; consequently, α_1 is $\mathcal{O}(1)$ (inset) and $\alpha_2 \ll 1$. Upon approaching the classical phase boundary, the ratio α_2/α_1 increases with $\alpha_1 \rightarrow 0$. The shaded region indicates the regime where a quantum spin liquid state has been reported at $h = 0$ [52]. The dotted (dashed) line is an extrapolation of the data toward \tilde{J}_{2c} (marks \tilde{J}_{2c}). Here, we have fixed $\tilde{J}_3 = 1/8$.

for a fixed μ_{eff}/J_1 at $d = 2$, as the system is tuned toward the LMCP from the canted Néel phase, the asymptotic scaling of $\rho_0 = [1/2 - \langle S^{(z)} \rangle]$ crosses over from $\rho_0 \sim (h_c - h) \rightarrow (h_c - h)^{1/2}$. We verify this crossover behavior through unbiased numerical calculations using infinite projected entangled-pair states (iPEPS) [63] as demonstrated in Fig. 3. We note that iPEPS works directly in the thermodynamic limits by exploiting translation invariance [64]. The accuracy of this variational ansatz is controlled by the bond dimension D of the tensors involved in their construction, which is related to the entanglement of the state.

Emergent algebraic liquid.—In order to understand the behavior of phase fluctuations at subcritical fields we introduce the hydrodynamic variables ϑ and ϱ , which represent the long-wavelength phase and density fluctuations, respectively, of boson field,

$$\Phi(\tau, \mathbf{r}) = \sqrt{\rho_0 + \varrho(\tau, \mathbf{r})} e^{i\vartheta(\tau, \mathbf{r})}. \quad (9)$$

For $\tilde{J}_2 < \tilde{J}_{2c}$ the FP state transitions into a canted Néel-AFM as h is lowered below h_c . This phenomenon is reflected in an U(1) symmetry breaking transition for the bosons, whereby $\langle \Phi \rangle \sim \sqrt{\rho_0} e^{-\frac{1}{2}i\vartheta^2} \neq 0$, which implies the existence of an ODLRO, hence a BEC [1,57]. As $\tilde{J}_2 \rightarrow \tilde{J}_{2c}$, the condensate fraction $\sim \langle \Phi \rangle$ is suppressed due to increased phase fluctuations. What is the fate of the system as $\langle \Phi \rangle \rightarrow 0$?

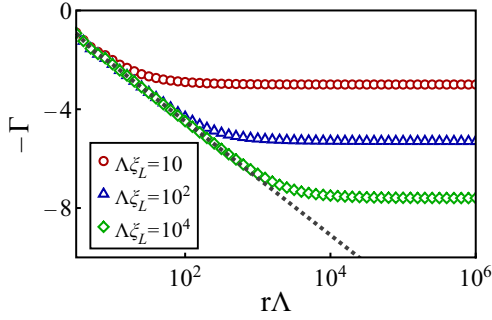


FIG. 4. Crossover behavior of $\langle S_0^{(+)} S_r^{(-)} \rangle$ as a function of r . For $|r|\Lambda \gg 1$ ($|r|\Lambda \ll 1$) the behavior is controlled by the canted-Néel phase (quantum critical point at $\tilde{J}_2 = \tilde{J}_{2c}$). The dotted line represents algebraic decay per Eq. (12). Here, $\xi_L \propto (\tilde{J}_{2c} - \tilde{J}_2)^{-1/2}$ and Λ^{-1} is a short-distance cutoff.

The dynamics of Φ , as dictated by S_M , is controlled by two independent length scales, $\rho_0^{-1/2}$ and $m_L^{-1/2}$. We fix the mean density ρ_0 (for fields $h < h_c$) and consider the influence of m_L (which controls proximity to CL_1) on the dynamics. The phase fluctuations are governed by the effective action [44]

$$S_g = \int \frac{dk_0 d\mathbf{k}}{(2\pi)^3} \left[\frac{k_0^2}{4g} + \rho_0 \varepsilon(\mathbf{k}, m_L) \right] \vartheta(-k) \vartheta(k), \quad (10)$$

where k_0 is the Euclidean frequency. We note that the propagator of ϑ is nonperturbative in g , and the phase fluctuations disperse as $\sqrt{4g\rho_0\varepsilon(\mathbf{k}, m_L)}$, which is analogous to the dispersion of magnons in the canted Néel phase. The long-wavelength behavior of the equal-time correlation function,

$$\langle S_0^{(+)} S_r^{(-)} \rangle \sim \langle \Phi^\dagger(0, \mathbf{0}) \Phi(0, \mathbf{r}) \rangle = \rho_0 \exp[-\Gamma(r, \xi_L)], \quad (11)$$

is determined by the correlation length $\xi_L \equiv \sqrt{A/m_L}$ through $\Gamma(r, \xi_L)$ [44]. The function $\Gamma(r, \xi_L)$ is most easily computed along the line $\gamma = \pi/4$, on which $\varepsilon(\mathbf{k}, m_L)$ acquires a C_∞ -rotational symmetry and $\xi_L \sim \sqrt{\tilde{J}_2/(1-4\tilde{J}_2)}$. As shown in Fig. 4, for $|r| \gg \xi_L$, $\langle S_0^{(+)} S_r^{(-)} \rangle$ saturates to a nonuniversal value (dependent on ρ_0 and ξ_L), implying the presence of ODLRO in Φ [65]. In the opposite limit, a universal scaling is obtained, indicating the presence of a quantum critical point (QCP) as $\xi_L \rightarrow \infty$ (dashed line in Fig. 4). This putative QCP is characterized by the absence of a BEC, i.e., $\langle \Phi \rangle = 0$. At small but finite T the canted Néel phase possesses only a quasi-long-range order, and goes through a Berezinskii-Kosterlitz-Thouless (BKT) transition upon raising T . Since the BKT transition scale T_{BKT} is controlled by m_L , it is expected to be suppressed as CL_1 is approached. Thus, the resultant crossover behavior is controlled by the critical fan

emanating from the critical point at $m_L = 0 \equiv \tilde{J}_2 = \tilde{J}_{2c}$ for $h < h_c$ [see Fig. 1(b)].

Interestingly, the QCP realizes a higher-dimensional analog of the Luttinger liquid, where a condensate cannot form due to strong infrared fluctuations. For sufficiently strong magnetic fields, and in the absence of proliferation of vortices of Φ [66], all points on CL_1 host such algebraic liquid states, which are parametrized by the critical exponent \mathcal{W} that controls the long-wavelength behavior of transverse spin correlations:

$$\langle S_0^{(+)} S_r^{(-)} \rangle \sim \rho_0 (|r|\Lambda)^{-\mathcal{W}}. \quad (12)$$

We find that $\mathcal{W} = \sqrt{g/(\rho_0 A)} f_w(\gamma)$, with f_w being a dimensionless function [44]. While generic points on CL_1 possess a C_4 rotational symmetry, a C_∞ symmetry emerges at $\gamma = \pi/4$, where CL_1 and CL_2 intersect (see Fig. 1). The C_∞ critical point would be expected to control the high-energy behavior in its vicinity, including that along CL_2 where a different kind of higher-dimensional Luttinger liquid is expected [4,67].

Conclusion.—Motivated by the ability of frustration to stabilize unconventional states of matter in quantum-spin systems, we studied its interplay with an applied magnetic field. With the help of the J_1 - J_2 - J_3 antiferromagnetic Heisenberg model, we demonstrated that frustration limits the validity of the BEC paradigm in describing the approach to saturation field. In particular, the phase transition between magnetically ordered and field-polarized states no longer belongs to the BEC universality class on the critical line CL_1 , along which frustration suppresses magnetic order. A similar outcome is expected along CL_2 and CL_3 , where the corresponding transitions are governed by distinct non-BEC universality classes.

In the vicinity of CL_1 , at subcritical fields, it is possible to realize bosonic quantum-liquid states that are stabilized by a combination of frustration and high magnetic fields. These quantum liquids are higher-dimensional analogs of gapless states that develop under sufficiently high magnetic fields in the spin-1 Haldane chain [21] and 1D valence bond solids [68]. We note that mechanisms similar to that described here may be responsible for stabilizing the quantum spin-liquid phase in the Kitaev honeycomb compass model in magnetic field along the [111] direction [69]. A detailed investigation into such possibilities is left to future works.

The authors thank Andrey Chubukov, Oleg Tchernyshyov, and Nandini Trivedi for fruitful discussions. The analytical work performed by S. S. and A. H. N. was supported by the U.S. Department of Energy Computational Materials Sciences (CMS) program under Award No. DE-SC0020177. The numerical calculations performed by Y. X. were supported by the U.S. National Science Foundation Division of Materials Research under Award

No. DMR-1917511. The computing resources at Rice University were supported in part by the Big-Data Private-Cloud Research Cyberinfrastructure MRI Award funded by NSF under Grant No. CNS-1338099 and by Rice University's Center for Research Computing (CRC). S. S. G. was supported by the NSFC (11834014, 11874078) and the Dongguan Key Laboratory of Artificial Intelligence Design for Advanced Materials. S. S. and A. H. N. are grateful for the hospitality of the Aspen Center for Physics, which is supported by National Science Foundation Grant No. PHY-2210452.

-
- [1] A. Leggett, Bose-Einstein condensation in the alkali gases: Some fundamental concepts, *Rev. Mod. Phys.* **73**, 307 (2001).
- [2] M. P. A. Fisher, P. B. Weichman, G. Grinstein, and D. S. Fisher, Boson localization and the superfluid-insulator transition, *Phys. Rev. B* **40**, 546 (1989).
- [3] A. Paramekanti, L. Balents, and M. P. A. Fisher, Ring exchange, the exciton Bose liquid, and bosonization in two dimensions, *Phys. Rev. B* **66**, 054526 (2002).
- [4] S. Sur and K. Yang, Metallic state in bosonic systems with continuously degenerate dispersion minima, *Phys. Rev. B* **100**, 024519 (2019).
- [5] H. C. Po and Q. Zhou, A two-dimensional algebraic quantum liquid produced by an atomic simulator of the quantum lifshitz model, *Nat. Commun.* **6**, 1 (2015).
- [6] A. Vishwanath, L. Balents, and T. Senthil, Quantum criticality and deconfinement in phase transitions between valence bond solids, *Phys. Rev. B* **69**, 224416 (2004).
- [7] E. Lake, M. Hermele, and T. Senthil, The dipolar Bose-hubbard model, *Phys. Rev. B* **106**, 064511 (2022).
- [8] H. Ma and M. Pretko, Higher-rank deconfined quantum criticality at the lifshitz transition and the exciton Bose condensate, *Phys. Rev. B* **98**, 125105 (2018).
- [9] J.-K. Yuan, S. A. Chen, and P. Ye, Fractonic superfluids, *Phys. Rev. Res.* **2**, 023267 (2020).
- [10] L. Balents, Spin liquids in frustrated magnets, *Nature (London)* **464**, 199 (2010).
- [11] O. A. Starykh, Unusual ordered phases of highly frustrated magnets: A review, *Rep. Prog. Phys.* **78**, 052502 (2015).
- [12] S. Beliaev, Energy spectrum of a non-ideal Bose gas, *Sov. Phys. JETP* **7**, 299 (1958), <http://jetp.ras.ru/cgi-bin/e/index/e/7/2/p299?a=list>.
- [13] T. Giamarchi, C. Rüegg, and O. Tchernyshyov, Bose-Einstein condensation in magnetic insulators, *Nat. Phys.* **4**, 198 (2008).
- [14] V. Zapf, M. Jaime, and C. D. Batista, Bose-Einstein condensation in quantum magnets, *Rev. Mod. Phys.* **86**, 563 (2014).
- [15] Y. Kamiya and C. D. Batista, Magnetic Vortex Crystals in Frustrated Mott Insulator, *Phys. Rev. X* **4**, 011023 (2014).
- [16] Z. Wang, Y. Kamiya, A. H. Nevidomskyy, and C. D. Batista, Three-dimensional crystallization of vortex strings in frustrated quantum magnets, *Phys. Rev. Lett.* **115**, 107201 (2015).
- [17] L. Balents and O. A. Starykh, Quantum lifshitz field theory of a frustrated ferromagnet, *Phys. Rev. Lett.* **116**, 177201 (2016).
- [18] S. Jiang, J. Romhányi, S. R. White, M. E. Zhitomirsky, and A. L. Chernyshev, Where is the quantum spin nematic?, *Phys. Rev. Lett.* **130**, 116701 (2023).
- [19] V. Galitski and I. B. Spielman, Spin-orbit coupling in quantum gases, *Nature (London)* **494**, 49 (2013).
- [20] H. Zhai, Degenerate quantum gases with spin-orbit coupling: A review, *Rep. Prog. Phys.* **78**, 026001 (2015).
- [21] S. Sachdev, T. Senthil, and R. Shankar, Finite-temperature properties of quantum antiferromagnets in a uniform magnetic field in one and two dimensions, *Phys. Rev. B* **50**, 258 (1994).
- [22] H. Tanaka, A. Oosawa, T. Kato, H. Uekusa, Y. Ohashi, K. Kakurai, and A. Hoser, Observation of field-induced transverse néel ordering in the spin gap system TiCuCl_3 , *J. Phys. Soc. Jpn.* **70**, 939 (2001).
- [23] N. Cavadini, C. Rüegg, A. Furrer, H.-U. Güdel, K. Krämer, H. Mutka, and P. Vorderwisch, Triplet excitations in low-h c spin-gap systems KCuCl_3 and TiCuCl_3 : An inelastic neutron scattering study, *Phys. Rev. B* **65**, 132415 (2002).
- [24] R. Coldea, D. A. Tennant, K. Habicht, P. Smeibidl, C. Wolters, and Z. Tylczynski, Direct measurement of the spin hamiltonian and observation of condensation of magnons in the 2d frustrated quantum magnet Cs_2CuCl_4 , *Phys. Rev. Lett.* **88**, 137203 (2002).
- [25] M. Jaime, V. F. Correa, N. Harrison, C. D. Batista, N. Kawashima, Y. Kazuma, G. A. Jorge, R. Stern, I. Heinmaa, S. A. Zvyagin *et al.*, Magnetic-field-induced condensation of triplons in lan purple pigment $\text{BaCuSi}_2\text{O}_6$, *Phys. Rev. Lett.* **93**, 087203 (2004).
- [26] A. Paduan-Filho, X. Gratens, and N. F. Oliveira Jr, Field-induced magnetic ordering in $\text{NiCl}_2 4\text{SC}(\text{NH}_2)_2$, *Phys. Rev. B* **69**, 020405(R) (2004).
- [27] T. Waki, M. Kato, Y. Itoh, C. Michioka, K. Yoshimura, and T. Goto, Triplon condensation of spin-gapped chain $\text{Pb}_2\text{V}_3\text{O}_9$, *J. Phys. Chem. Solids* **66**, 1432 (2005).
- [28] T. Nakajima, H. Mitamura, and Y. Ueda, Singlet ground state and magnetic interactions in new spin dimer system $\text{Ba}_3\text{Cr}_2\text{O}_8$, *J. Phys. Soc. Jpn.* **75**, 054706 (2006).
- [29] V. O. Garlea, A. Zheludev, T. Masuda, H. Manaka, L.-P. Regnault, E. Ressouche, B. Grenier, J.-H. Chung, Y. Qiu, K. Habicht *et al.*, Excitations from a Bose-Einstein condensate of magnons in coupled spin ladders, *Phys. Rev. Lett.* **98**, 167202 (2007).
- [30] A. Kitada, Z. Hiroi, Y. Tsujimoto, T. Kitano, H. Kageyama, Y. Ajiro, and K. Yoshimura, Bose-Einstein condensation of quasi-two-dimensional frustrated quantum magnet $(\text{CuCl})\text{LaNb}_2\text{O}_7$, *J. Phys. Soc. Jpn.* **76**, 093706 (2007).
- [31] M. B. Stone, C. Broholm, D. H. Reich, P. Schiffer, O. Tchernyshyov, P. Vorderwisch, and N. Harrison, Field-driven phase transitions in a quasi-two-dimensional quantum antiferromagnet, *New J. Phys.* **9**, 31 (2007).
- [32] V. O. Garlea, A. Zheludev, K. Habicht, M. Meissner, B. Grenier, L.-P. Regnault, and E. Ressouche, Dimensional crossover in a spin-liquid-to-helimagnet quantum phase transition, *Phys. Rev. B* **79**, 060404(R) (2009).
- [33] A. A. Aczel, Y. Kohama, C. Marcenat, F. Weickert, M. Jaime, O. E. Ayala-Valenzuela, R. D. McDonald,

- S. D. Selesnic, H. A. Dabkowska, and G. M. Luke, Field-induced Bose-Einstein condensation of triplons up to 8K in $\text{Sr}_3\text{Cr}_2\text{O}_8$, *Phys. Rev. Lett.* **103**, 207203 (2009).
- [34] A. A. Tsirlin, R. Nath, F. Weickert, Y. Skourski, C. Geibel, and H. Rosner, Magnetic interactions and high-field properties of $\text{Ag}_2\text{VOP}_2\text{O}_7$: frustrated alternating chain close to the dimer limit, *J. Phys. Conf. Ser.* **145**, 012067 (2009).
- [35] B. Thielemann, C. Rüegg, K. Kiefer, H. M. Rønnow, B. Normand, P. Bouillot, C. Kollath, E. Orignac, R. Citro, T. Giamarchi *et al.*, Field-controlled magnetic order in the quantum spin-ladder system $(\text{Hpip})_2\text{CuBr}_4$, *Phys. Rev. B* **79**, 020408(R) (2009).
- [36] E. C. Samulon, Y. Kohama, R. D. McDonald, M. C. Shapiro, K. A. Al-Hassanieh, C. D. Batista, M. Jaime, and I. R. Fisher, Asymmetric quintuplet condensation in the frustrated $S = 1$ spin dimer compound $\text{Ba}_3\text{Mn}_2\text{O}_8$, *Phys. Rev. Lett.* **103**, 047202 (2009).
- [37] I. Bostrem, V. Sinitsyn, A. Ovchinnikov, Y. Hosokoshi, and K. Inoue, Bose-Einstein condensation of semi-hard bosons in the $S = 1$ dimerized organic compound F2PNNNO, *J. Phys. Condens. Matter* **22**, 036001 (2009).
- [38] T. Hong, C. Stock, I. Cabrera, C. Broholm, Y. Qiu, J. B. Leao, S. J. Poulton, and J. R. D. Copley, Neutron scattering study of a quasi-two-dimensional spin-1/2 dimer system: Piperazine hexachlorodocuprate under hydrostatic pressure, *Phys. Rev. B* **82**, 184424 (2010).
- [39] A. A. Tsirlin, R. Nath, J. Sichelschmidt, Y. Skourski, C. Geibel, and H. Rosner, Frustrated couplings between alternating spin-1/2 chains in AgVOAsO_4 , *Phys. Rev. B* **83**, 144412 (2011).
- [40] K. M. Ranjith, D. Dmytriieva, S. Khim, J. Sichelschmidt, S. Luther, D. Ehlers, H. Yasuoka, J. Wosnitza, A. A. Tsirlin, H. Kühne, and M. Baenitz, Field-induced instability of the quantum spin liquid ground state in the $J_{\text{eff}} = \frac{1}{2}$ triangular lattice compound NaYbO_2 , *Phys. Rev. B* **99**, 180401(R) (2019).
- [41] K. M. Ranjith, S. Luther, T. Reimann, B. Schmidt, P. Schlender, J. Sichelschmidt, H. Yasuoka, A. M. Strydom, Y. Skourski, J. Wosnitza, H. Kühne, T. Doert, and M. Baenitz, Anisotropic field-induced ordering in the triangular-lattice quantum spin liquid NaYbSe_2 , *Phys. Rev. B* **100**, 224417 (2019).
- [42] T. Halloran, F. Desrochers, E. Z. Zhang, T. Chen, L. E. Chern, Z. Xu, B. Winn, M. Graves-Brook, M. Stone, A. I. Kolesnikov *et al.*, Geometrical frustration versus Kitaev interactions in $\text{BaCo}_2(\text{AsO}_4)_2$, *Proc. Natl. Acad. Sci. U.S.A.* **120**, e2215509119 (2023).
- [43] X. Zhang, Y. Xu, T. Halloran, R. Zhong, C. Broholm, R. J. Cava, N. Drichko, and N. P. Armitage, A magnetic continuum in the cobalt-based honeycomb magnet $\text{BaCo}_2(\text{AsO}_4)_2$, *Nat. Mater.* **22**, 58 (2023).
- [44] See Supplemental Material at <http://link.aps.org/supplemental/10.1103/PhysRevLett.132.066701> for the derivation of the effective models, RG calculations, background calculations for the phase diagrams, and details of the iPEPS calculations.
- [45] M. W. Butcher, M. A. Tanatar, and A. H. Nevidomskyy, Anisotropic melting of frustrated Ising antiferromagnets, *Phys. Rev. Lett.* **130**, 166701 (2023).
- [46] Two other critical lines are present in the phase diagram: CL_2 (CL_3) separates the two spiral-ordered (stripe-ordered and spiral ordered) phases. Here, we primarily focus on the impact of CL_1 on the phase diagram.
- [47] L. Capriotti and S. Sachdev, Low-temperature broken-symmetry phases of spiral antiferromagnets, *Phys. Rev. Lett.* **93**, 257206 (2004).
- [48] Y. A. Kharkov, J. Oitmaa, and O. P. Sushkov, Properties of the spin-liquid phase in the vicinity of the Lifshitz transition from n el to spin-spiral state in frustrated magnets, *Phys. Rev. B* **98**, 144420 (2018).
- [49] J. Reuther, P. W ofle, R. Darradi, W. Brenig, M. Arlego, and J. Richter, Quantum phases of the planar antiferromagnetic $J_1 - J_2 - J_3$ Heisenberg model, *Phys. Rev. B* **83**, 064416 (2011).
- [50] P. Sindzingre, N. Shannon, and T. Momoi, Phase diagram of the spin-1/2 $J_1 - J_2 - J_3$ Heisenberg model on the square lattice, *J. Phys. Conf. Ser.* **200**, 022058 (2010).
- [51] S.-S. Gong, W. Zhu, D. N. Sheng, O. I. Motrunich, and M. P. A. Fisher, Plaquette ordered phase and quantum phase diagram in the spin-1/2 $J_1 - J_2$ square Heisenberg model, *Phys. Rev. Lett.* **113**, 027201 (2014).
- [52] W.-Y. Liu, J. Hasik, S.-S. Gong, D. Poilblanc, W.-Q. Chen, and Z.-C. Gu, Emergence of gapless quantum spin liquid from deconfined quantum critical point, *Phys. Rev. X* **12**, 031039 (2022).
- [53] M. Wu, S.-S. Gong, D.-X. Yao, and H.-Q. Wu, Phase diagram and magnetic excitations of $J_1 - J_3$ Heisenberg model on the square lattice, *Phys. Rev. B* **106**, 125129 (2022).
- [54] T. Matsubara and H. Matsuda, A lattice model of liquid helium, I, *Prog. Theor. Phys.* **16**, 569 (1956).
- [55] E. G. Batyev and L. S. Braginskii, Antiferromagnet in a strong magnetic field: Analogy with Bose gas, *Sov. Phys. JETP* **60**, 781 (1984), <http://jetp.ras.ru/cgi-bin/e/index/e/60/4/p781?a=list>.
- [56] The existence of such a Lifshitz transition is directly diagnosed by the low-energy density of states, which acquires a more singular energy scaling at a Lifshitz critical point than the abutting phases.
- [57] O. Penrose and L. Onsager, Bose-Einstein condensation and liquid helium, *Phys. Rev.* **104**, 576 (1956).
- [58] S. Sachdev, *Quantum Phase Transitions* (Cambridge University Press, Cambridge, England, 2011).
- [59] S. Sachdev, Quantum phase transitions and conserved charges, *Z. Phys. B* **94**, 469 (1994).
- [60] X.-G. Wen, Chiral Luttinger liquid and the edge excitations in the fractional quantum hall states, *Phys. Rev. B* **41**, 12838 (1990).
- [61] S. Sur and S.-S. Lee, Chiral non-Fermi liquids, *Phys. Rev. B* **90**, 045121 (2014).
- [62] D. S. Fisher and P. C. Hohenberg, Dilute Bose gas in two dimensions, *Phys. Rev. B* **37**, 4936 (1988).
- [63] J. Hasik and G. B. Mbeng, peps-torch: A differentiable tensor network library for two-dimensional lattice models, <https://github.com/jurajHasik/peps-torch>.
- [64] J. Jordan, R. Or s, G. Vidal, F. Verstraete, and J. I. Cirac, Classical simulation of infinite-size quantum lattice systems in two spatial dimensions, *Phys. Rev. Lett.* **101**, 250602 (2008).

- [65] We clearly observe a suppression of the condensate fraction as CL_1 is approached (i.e. $\xi_L \rightarrow \infty$).
- [66] The arguments against the relevance of global vortices at $T = 0$ that were developed in Ref. [67] are expected to be applicable here, because the ring-minima is smoothly connected to the $\gamma = \pi/4$ point on CL_1 as its radius shrinks to zero.
- [67] E. Lake, T. Senthil, and A. Vishwanath, Bose-luttinger liquids, *Phys. Rev. B* **104**, 014517 (2021).
- [68] A. Iaizzi and A. W. Sandvik, 1d valence bond solids in a magnetic field, *J. Phys. Conf. Ser.* **640**, 012043 (2015).
- [69] N. D. Patel and N. Trivedi, Magnetic field-induced intermediate quantum spin liquid with a spinon fermi surface, *Proc. Natl. Acad. Sci. U.S.A.* **116**, 12199 (2019).